# A universal strategy for visually guided landing

Emily Baird[a,1], Norbert Boeddeker[b], Michael R. Ibbotson[c,d], and Mandyam V. Srinivasan[e,f]

[a]Department of Biology, Lund University, S-2232 Lund, Sweden; [b]Department of Cognitive Neurosciences, Bielefeld University, D-33501 Bielefeld, Germany; [c]National Vision Research Institute, Australian College of Optometry, Carlton, VIC 3053, Australia; [d]Department of Optometry and Vision Science, University of Melbourne, Melbourne, VIC 3010, Australia; [e]Queensland Brain Institute and School of Information Technology and Electrical Engineering, The University of Queensland, St. Lucia, QLD 4072, Australia; and [f]Australian Research Council Centre for Excellence in Vision Science, Australian National University, Canberra, ACT 2600, Australia

Edited by John G. Hildebrand, University of Arizona, Tucson, AZ, and approved September 24, 2013 (received for review July 31, 2013)

**Landing is a challenging aspect of flight because, to land safely, speed must be decreased to a value close to zero at touchdown. The mechanisms by which animals achieve this remain unclear. When landing on horizontal surfaces, honey bees control their speed by holding constant the rate of front-to-back image motion (optic flow) generated by the surface as they reduce altitude. As inclination increases, however, this simple pattern of optic flow becomes increasingly complex. How do honey bees control speed when landing on surfaces that have different orientations? To answer this, we analyze the trajectories of honey bees landing on a vertical surface that produces various patterns of motion. We find that landing honey bees control their speed by holding the rate of expansion of the image constant. We then test and confirm this hypothesis rigorously by analyzing landings when the apparent rate of expansion generated by the surface is manipulated artificially. This strategy ensures that speed is reduced, gradually and automatically, as the surface is approached. We then develop a mathematical model of this strategy and show that it can effectively be used to guide smooth landings on surfaces of any orientation, including horizontal surfaces. This biological strategy for guiding landings does not require knowledge about either the distance to the surface or the speed at which it is approached. The simplicity and generality of this landing strategy suggests that it is likely to be exploited by other flying animals and makes it ideal for implementation in the guidance systems of flying robots.**

vision | flight control | insect | three-dimensional surface

Orchestrating a safe landing is one of the greatest challenges for flying animals and airborne vehicles alike. Although some progress has been made toward unraveling the cues that flying animals might use for triggering landings (1–10), we do not yet have a good understanding of how these or other possible cues are used to control the landing process once it has been initiated.

To achieve a smooth landing, it is essential to control deceleration in such a manner that the approach speed decreases to a value close to zero at the time of touchdown. An obvious way to achieve this would be to measure flight speed and distance to the target simultaneously and to use this information to reduce speed progressively, in a moment-to-moment fashion. However, this strategy is computationally demanding and unsuitable for animals such as flying insects, whose close-set, fixed-focus eyes prevent them from using stereopsis or accommodation to measure the distances to surfaces directly (11–13).

When performing a grazing landing on a horizontal surface, honey bees use a technique that allows them to overcome the limitations of their relatively simple nervous systems. Instead of measuring the distance to the surface directly, they hold constant the magnitude of optic flow (the speed of image motion on the retina) that is generated by the ground beneath them (4, 5). This automatically ensures that the speed of flight is reduced as the ground is approached, reaching a value very close to zero at touchdown.

Grazing approaches, however, constitute a special, restricted class of landings in which the direction of motion is almost parallel to the surface. The pattern of optic flow produced by this type of landing is almost purely translatory in structure—all regions of the ground seem to move in the same front-to-back direction. However, in the natural world, bees would only occasionally make such grazing landings on flat surfaces. A perpendicular approach to the surface of a flower, for example, would generate an entirely different and more complex pattern of optic flow, namely, one of radial expansion, in which the various regions of the image move radially outward from the point that is being approached (14, 15). It is important, therefore, to ask whether bees—and flying animals in general—possess a universal landing strategy that can operate in a variety of circumstances, including approaches to horizontal, vertical, and oblique surfaces, as well as small, raised objects such as flowers. Here we address this question by asking how bees approach and land on a vertically oriented surface.

## Results

**Exp. 1: Basic Properties of Landing Approaches.** Honey bees were trained to collect a food reward by flying toward a small aperture (1.5 cm in diameter) in the center of a vertical disk, 60 cm in diameter, to access a food reward positioned behind it (*SI Appendix*, Fig. S1).

We began by filming the trajectories of bees approaching a vertically oriented checkerboard pattern (Fig. 1, *Inset*). The bees approached the pattern in a direction perpendicular to the surface, with little variation in either the vertical or horizontal component of their flight path (Fig. 1).

How does the approach speed vary with the distance to the target? This relationship is shown in Fig. 2 for approach flights toward each of three different patterns: checkerboard, concentric rings, and sectors (Fig. 2, *Insets*). We find that the average approach speed decreases approximately linearly as a function of target distance: The closer the target, the slower the approach speed. When the bees are close (under 7 cm) to the surface, they

### Significance

**In this study, we investigate the cues that honey bees use to land on vertical surfaces. We show that bees use the apparent rate of expansion of the image generated by the surface to smoothly reduce their speed when landing. From our results, we develop a mathematical model for visually guided landing that, unlike all current engineering-based methods, does not require knowledge about either the distance to the surface or the speed at which it is approached. This strategy is not only specific to landings on vertical surfaces or to honey bees but represents a universal strategy that any flying agent (animal or machine) could use to land safely on surfaces of any orientation.**

Author contributions: E.B., M.R.I., and M.V.S. designed research; E.B. performed research; N.B. and M.R.I. contributed new methods; E.B. analyzed data; and E.B., N.B., and M.V.S. wrote the paper.

The authors declare no conflict of interest.

This article is a PNAS Direct Submission.

[1]To whom correspondence should be addressed. E-mail: emily.baird@biol.lu.se.

This article contains supporting information online at www.pnas.org/lookup/suppl/doi:10.1073/pnas.1314311110/-/DCSupplemental.

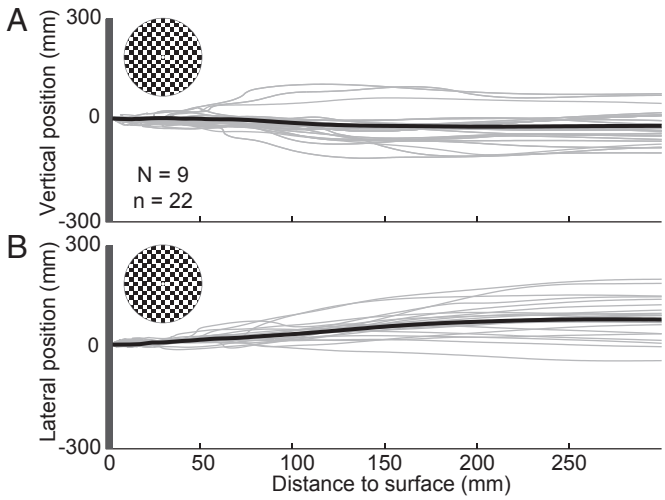


**Fig. 1** Flights of bees approaching the checkerboard pattern (gray vertical line and *Inset*) as viewed from the side (*A*) and from above (*B*). The black line in each panel shows the mean trajectory. The feeder tube is at 0 mm. N denotes the number of individuals; n denotes the number of flights.

enter a short hover phase before touchdown, a behavior previously described in ref. 16. This final landing phase did not vary between the conditions, probably because the landing tube would provide strong visual cues at this distance, and was therefore not included in our analysis.

In Fig. 2 and all subsequent figures, we plot the axial component of the approach speed (the speed along a direction, $z$, perpendicular to the plane of the disk), rather than the total speed. The reason is that it is this component of the speed that needs to be reduced progressively as the surface is approached. However, all of the results are essentially unaltered if we consider the 3D speed, rather than the axial speed, due to the perpendicular direction of the approaches (Fig. 1). Henceforth, we will simply refer to the axial component of the bee's speed as the "approach speed" or "flight speed."

What is the nature of the visual stimulus that a honey bee would perceive when it approaches a pattern at a speed that is proportional to its distance from the pattern? Consider a bee flying at a speed $V$, approaching a stationary vertical surface at a distance $z$, in a direction perpendicular to the plane of the surface (*SI Appendix*, Fig. S2). The apparent value of the angular velocity $\frac{d\theta}{dt}$ of a point on the surface that is viewed by the bee's eye along an angle $\theta$ from the forward direction is given by

$$\frac{d\theta}{dt} = \frac{V}{2z} \cdot sin2\theta. \qquad [1]$$

The angular velocity will vary with the viewing direction and will be highest at a direction of 45° (because sin $2\theta$ is maximum when $2\theta = 90°$), irrespective of the bee's approach speed or its distance from the surface (details of the derivation are given in *SI Appendix*, Text S1).

To explore the significance of the angular velocity of the image, we rewrite Eq. **1** as

$$\frac{V}{z} = 2\frac{\left(\frac{d\theta}{dt}\right)}{sin2\theta}. \qquad [2]$$

Eq. **2** reveals that if the bee adjusts its approach speed $V$ in such a way that the angular velocity of the image $\frac{d\theta}{dt}$ in a given viewing direction $\theta$ is always constant, then the ratio $V/z$ will be constant, which implies that the speed of approach will be proportional to the target distance. Thus, in principle, the bee can progressively reduce its speed during the approach simply by holding constant the angular velocity that is generated by a point on the surface in a particular viewing direction. This result is independent of the viewing direction (or directions) along which the bee measures and regulates the image angular velocity. Indeed, the same landing behavior would result if the bee were to hold constant the entire image velocity profile (image velocities measured in various viewing directions), or the sum of the local image speeds measured within a circumscribed visual field. All of these quantities would be measures of the rate of expansion of the image, which the bee would have to hold constant to land in the observed manner.

Are bees using image expansion as a cue to achieve a smooth landing? Fig. 2 offers some evidence that this may indeed be the case. When the pattern provides strong image-expansion cues [as in the case of the checkerboard (Fig. 2*A*) or the concentric rings (Fig. 2*B*)], the various flight speed profiles are quite consistent and are clustered around the mean profile (dark gray lines). However, with the sector pattern (Fig. 2*C*), which provides weak or no expansion cues (because the radial edges of the sectors do not seem to move when the image expands) the speed profiles are much more variable. In this case some bees do not even begin to slow down until they are very close to the pattern, and others approach the pattern at a more or less constant speed. This suggests that the ability to decelerate appropriately to perform a smooth landing is compromised when the cues that reveal image expansion are impoverished.

**Exp. 2: Landing Approaches Toward Stationary and Rotating Spirals.** A possible explanation for the results of Exp. 1 is that honey bees control their approach speed by holding constant the rate of expansion of the image when landing on a vertical surface. One way to test this hypothesis critically would be to examine the consequences of artificially manipulating the rate of image expansion that they experience when approaching a vertical surface. This can be achieved using a specially constructed spiral pattern that, when rotated, either increases or decreases the

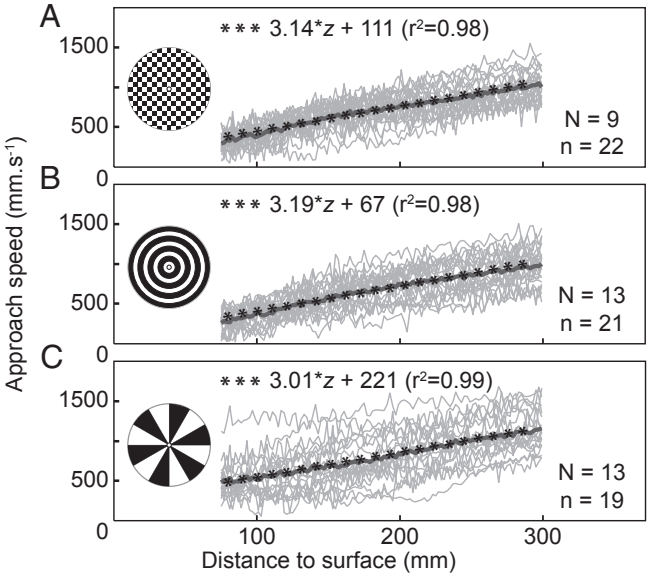


**Fig. 2** The relationship between approach speed and distance from the surface of bees approaching a checkerboard (*A*), concentric ring (*B*), or sector (*C*) pattern. Light gray lines represent individual flight data; dark gray lines indicate the mean of all flights and starred lines represent linear regressions of the mean data, as specified by the equation in each panel. N denotes the number of individuals; n denotes the number of flights.

magnitude of the expansional optic flow that the bee would perceive as it approached the target, without distorting the profile of the expansion (*SI Appendix*, Text S2).

If bees achieve smooth landings by holding constant the rate of expansion of the frontal image, we can predict how they should behave when they approach our rotating spiral. Our mathematical model (*SI Appendix*, Texts S3 and S4) predicts that the rotation of the spiral should change the slope of the relationship between the approach velocity and target distance according to the expression

$$\frac{V_{rot}}{z} = \frac{V_{stat}}{z} - B\omega, \qquad [3]$$

where $V_{stat}$ is the velocity of approach toward a stationary spiral, $V_{rot}$ is the velocity of approach toward a rotating spiral, $z$ is target distance, $B$ is the pitch of the spiral (0.3), and $\omega$ is the angular velocity of its rotation (rad·s$^{-1}$; *SI Appendix*, Text S4). $\omega$ is positive when the rotation is in a direction to generate apparent expansion and negative when the rotation generates contraction. Eq. **3** predicts that when the spiral is rotating, the approach speed $V_{rot}$ will continue to be proportional to target distance $z$, but the slope of this relationship $\frac{V_{rot}}{z}$ will be lower or higher than that for the stationary spiral $\frac{V_{stat}}{z}$ by the amount $B\omega$, depending upon whether the spiral is generating expansion or contraction.

To test the predictions of our mathematical model, we recorded the approach trajectories of bees when the disk displayed a four-arm spiral pattern that was either stationary or rotating at speeds of 0.5 or 1 rotation per second (rps), either in the counterclockwise or the clockwise direction, so as to increase or decrease the apparent rate of expansion, respectively (Fig. 3).

Fig. 3*B* shows the maximum angular velocity (the angular velocity at a viewing direction of 45°) that would be perceived by the landing honey bees as a function of their distance from the disk, for each rotational speed of the expanding spiral. This figure reveals that angular velocity is held at a relatively constant value, irrespective of the bee's distance from the disk. Evidently, regardless of whether the spiral is stationary or expanding at 0.5 or 1 rps, the honey bees are adjusting their approach speed so as to keep the maximum angular velocity (or, equally, the angular velocity at any particular viewing angle) of the radial expansion of the spiral nearly constant during the entire approach. In these experimental conditions, the bees were holding the maximum angular velocity relatively constant at values between 90°·s$^{-1}$ and 160°·s$^{-1}$ during the approach.

The black dotted curve in Fig. 3 *B* and *D* is a prediction of the increase in angular velocity that a honey bee would experience if it approached a stationary spiral at a constant speed corresponding to its initial speed (1,018 mm·s$^{-1}$), without any deceleration. This curve was computed from *SI Appendix*, Eq. S21 by setting $\theta = 45°$, $B = 0.3$, $V = 1{,}018$ mm·s$^{-1}$, and $\omega = 0$. The large difference between this theoretical curve and the angular velocities that the honey bees actually experience during the landing indicates that, for each speed of spiral expansion, the bees are doing a very good job of adjusting their approach speed to maintain a constant rate of image expansion throughout the landing.

Fig. 3*C* shows the variation of approach speed with distance for contracting spirals. As with the response to expanding spirals, this relationship can again be approximated by a linear regression, but fitted over a shorter range than for the expanding spirals, between 75 and 210 mm for 0.5 rps and between 75 and 120 mm for 1 rps (the upper limits were determined by finding the distance over which the variation in the data were best described by the linear fit as determined by the distance at which the $r^2$ value was maximal). As we shall discuss later, this indicates that the onset of the landing phase is delayed because of the reduced rate of image expansion caused by the contracting spirals.

Fig. 3*D* shows the variation of the maximum angular velocity that would be perceived by the landing honey bees when the spiral is contracting. At the lowest rotational speed (0.5 rps), the bees maintain this angular velocity constant at a value of about 100°·s$^{-1}$ (blue line), just as they do in the case of the stationary spiral (black line) and the expanding spirals (Fig. 3*B*). At 1 rps, the angular velocity shows some variation through the course of

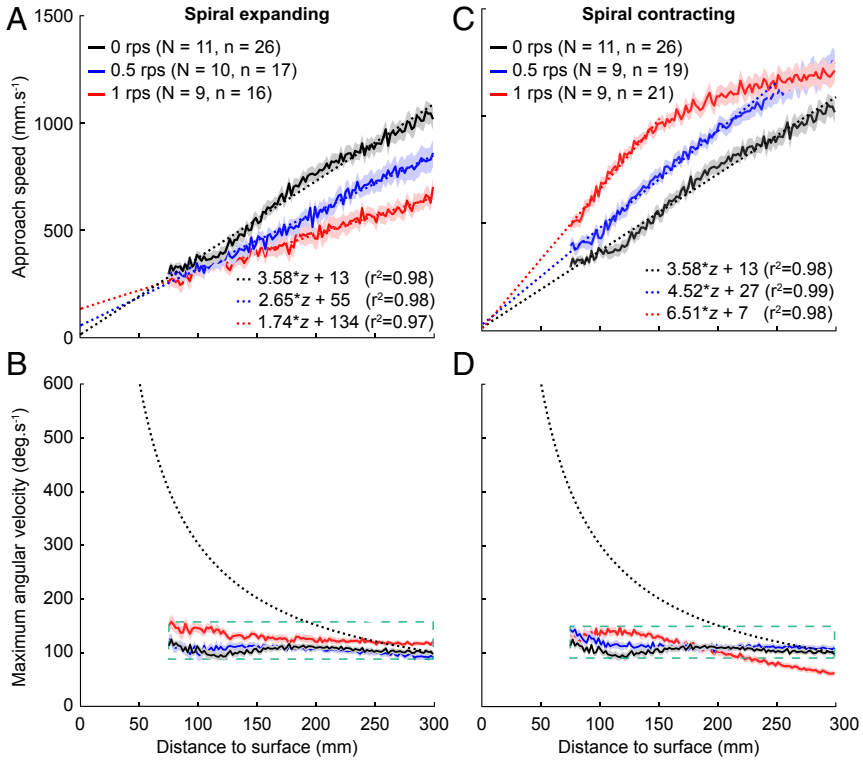


**Fig. 3** (*A*) Variation of speed with distance to the surface as honey bees approach a four-arm spiral that is stationary, expanding at 0.5 or 1 rps (black, blue, and red data, respectively). Solid lines show the mean response; shaded areas indicate the SEM. Dotted lines indicate linear regressions of the mean data as specified by the equations. (*B*) Maximum image angular velocity that bees experience as they approach the spiral at each rotational speed. The black dotted line indicates the expected variation of the maximum angular velocity with the distance to the surface if the bees were to approach a stationary spiral at a constant speed corresponding to their initial approach speed. The green dashed box depicts the range of mean maximum angular velocities that are experienced during the landing phase in all conditions. (*C*) Data from experiments with details as in *A* but using contracting spirals. The data for the stationary spiral (black line) is repeated from *A* to facilitate comparison. In this case, the linear regressions for 0.5 (blue dotted line) and 1 rps (red dotted line) have been fitted to data for distances lower than 210 mm and 120 mm, respectively, as explained in the text. (*D*) Data from experiments with details as in *B* but using contracting spirals.

the trajectory. This can be explained if we postulate that the landing phase is fully initiated only when the bee has approached to within about 120 mm of the target. At greater distances the bee is gradually transitioning from a "cruise" mode to a "landing" mode, as is evident from Fig. 3*C*.

With the contracting spirals, the model prediction is that the slope of the speed versus distance curve should progressively increase as the rotational speed of the spiral is increased. This is evident from Fig. 3*C*. Table 1 shows that the predicted slopes are in excellent agreement with those observed, for expanding as well as contracting spirals.

**Exp. 3: Effect of Temporal Frequency on Approach Speed During Landing.** To investigate whether landing honey bees control the speed of their approach by measuring the temporal frequency generated by the pattern—rather than the apparent rate of expansion—we filmed landing trajectories for spiral patterns of various spatial frequencies. A spiral with a higher spatial frequency would generate a higher temporal frequency of intensity fluctuations in the photoreceptors, compared with a spiral with a lower spatial frequency rotating at the same speed. The spirals used in this experiment had three, four, or six arms (*SI Appendix*, Fig. S1*C*). The effect of each of the spirals on approach speed was tested when the disk was stationary and when it was rotating either counterclockwise (increasing the rate of radial expansion) or clockwise (decreasing the rate of radial expansion) at 1 rps. Fig. 4 shows the relationship between approach speed and target distance for the three different spirals for each condition of pattern rotation.

For all conditions of rotation, the variation of approach speed with distance is similar for all three spirals (Fig. 4). This relationship is also similar to that observed in Exp. 2 (Fig. 3 *A* and *C*) in the equivalent conditions. These findings suggest that landing is controlled by a motion-sensing system that measures the angular velocity of expansion of the image, irrespective of the temporal frequency that it generates in the visual system.

## Discussion

In this study we examine how honey bees achieve smooth landings on vertical surfaces. Specifically, we have shown that smooth deceleration and a gentle touchdown are achieved by keeping constant some measure of the rate of expansion of the image of the surface that is being approached. This surprisingly elegant strategy for guiding landings does not require knowledge of the distance to the surface, or of the speed of approach—it only requires measurement of the rate of expansion of the image of the surface. Because image expansion is the only cue that is required, an added advantage of this strategy is that it does not require a constant attitude in pitch, roll, or yaw.

Our theoretical model of this process predicts that approach speed should decrease linearly with distance from the surface and reach a value close to zero at contact. For stationary spirals, this prediction is borne out by the data (Fig. 3). For expanding spirals, the relationship between approach speed and distance is very consistent with model predictions—the approach speed again decreases linearly with target distance, but at a lower rate when the rotational speed of the spiral is increased (Table 1).

**Table 1. Measured and theoretical relationships between approach speed and distance to the surface when the spiral is stationary (S), expanding (E), or contracting (C)**

| Spiral rotation, rps | Predicted change of slope due to spiral rotation ($B\omega$) | Predicted slope (stationary slope – $B\omega$) | Slope from data | Difference between observed and predicted values |
|---|---|---|---|---|
| S | 0 | — | 3.58 | — |
| E 0.5 | 0.94 | 2.64 | 2.65 | 0.01 (0.38%) |
| E 1 | 1.88 | 1.70 | 1.74 | 0.04 (2.35%) |
| C 0.5 | −0.94 | 4.52 | 4.52 | 0.00 (0.00%) |
| C 1 | −1.88 | 6.41 | 6.54 | 0.13 (2.03%) |

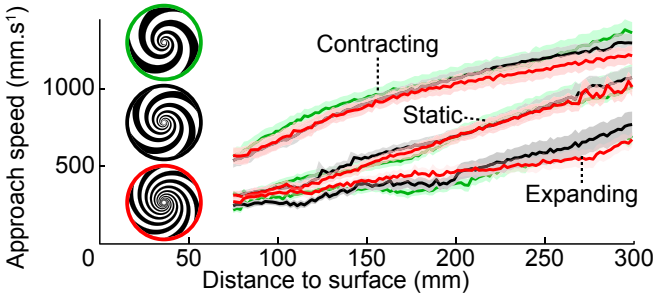


**Fig. 4** Variation of speed with distance to the surface for spirals of different spatial frequency when the spiral is stationary, contracting or expanding at 1 rps, and when it has three, four, or six arms (green, black and red lines, respectively). Solid lines show the mean response; shaded areas indicate the SEM. The number of flights for the stationary, expanding, and contracting spirals is, respectively, 19, 22, and 21; 21, 22, and 20; and 20, 23, and 22 for the three-, four-, and six-arm spirals, respectively.

When confronted with contracting spirals (Fig. 3*C*), the relationship between approach speed and target distance is best approximated by linear regressions that start closer to the surface than for the stationary or expanding spirals. At the highest speed of rotation, bees approach the spiral at an approximately constant speed until they have come closer to the target. Presumably this is because the net image expansion experienced by the visual system is so weak (because of the cancellation by the contracting spiral) that it does not trigger the landing phase until the bee has reached a certain target distance. Our model is also successful at predicting the behavior of bees when they approach contracting spirals, once they have entered the landing phase.

The results of Exp. 3 reveal that the approach speed profile is not affected by changes in the spatial structure of the spiral pattern. This reinforces our hypothesis that honey bees regulate their speed during landing by holding constant some component of the angular velocity profile of the image when they approach a vertical surface. This finding is congruent with the results of earlier investigations which have shown that the visual mechanisms that mediate other honey bee flight behaviors—such as the centering response (17), visual odometry (18, 19), and control of cruising speed (20)—are sensitive to the angular velocity of the image, and not to its spatial or temporal frequency content. If the visual mechanism that guides landing were sensitive to these individual parameters, then the speed of approach would depend not only upon the angular velocity of the image but also upon the textural properties of the surface, and therefore prevent consistently smooth and safe landings. By measuring the angular velocity profile of the image of the landing surface—largely independently of its spatial-frequency or temporal-frequency content—it is possible to ensure that the speed of approach during landing is regulated according to the distance to the surface, regardless of its spatial texture.

**How Do Honey Bees Know When to Land?** Honey bees maintain a constant forward speed during cruising flight by holding constant the angular velocity of the image of the environment on their retina (18, 20). When a similar strategy is applied to the optic flow generated by a surface that is approached for landing, the speed of approach would gradually be reduced to a value close to zero near the surface. What cues do honey bees use to initiate the transition from cruising flight to landing? When a surface is being approached, landing could be initiated when the magnitude of the optic flow (i.e., the rate of expansion) that is

generated by the surface reaches a threshold value. If this were the case, one would expect landings to be initiated closer to the target when the rate of expansion of the image is artificially decreased. Qualitatively, this is what we observe in the experiments with the contracting spirals, although further work is required to test this quantitatively.

**What Are the Cues That Are Used to Guide Landing?** Which particular aspect of image expansion do honey bees measure and hold constant when they are landing? Any of a variety of parameters that signal the rate of image expansion would elicit the observed behavior (*SI Appendix*, Text S5). Potential cues could be, for example, the magnitude of the optic flow as measured in a particular viewing direction, or the maximum magnitude of optic flow (generated anywhere in the image), or the summed magnitudes of the optic flow vectors integrated over a cone of the frontal visual field. Our experiments do not allow us to distinguish between these possibilities, because all of them would generate the same behavior. Nonetheless, our modeling indicates that the approach speed will decrease proportionally to target distance as long as any of these measures of the rate of image expansion is held constant as the surface is approached. This strategy would function not only for landing on vertical surfaces, but also on surfaces of any orientation (including horizontal surfaces), and for any direction of approach. The mathematical proof of this is given in *SI Appendix*, Text S5, where it is shown that the strategy can also be applied to landing on a variety of other 3D objects, such as ridges or flower-like structures.

Our experiments and modeling should help guide searches for the neural circuits that underlie control of landing by specifying the response properties that they are likely to possess. For example, deceleration during landing could be guided by adjusting flight speed in such a way that the output of a visual interneuron, which sums the magnitudes of the responses of a number of small-field ("elementary") motion detectors, is held constant. Thus, the strategy of holding constant some measure of the optic flow profile that is generated by the surface represents a universal, computationally efficient scheme for guiding landings that could be used by any flying animal or machine.

**Other Models of Visual Guidance for Landing.** A study by Wagner (7) and, more recently, a detailed investigation by van Breugel and Dickinson (6) have suggested that, in flies, prelanding deceleration is initiated when the ratio of the angular size of the image to its angular rate of expansion falls below a critical value. This ratio, known as *Tau*, is equal to the projected time to contact with the surface, if the fly were to continue to move toward the surface at the same speed (21). The value of *Tau* provides useful information about when to initiate a landing response. However, the computed value of *Tau* does not, on its own, prescribe the way in which a flying insect should reduce its speed to achieve a gentle touchdown—it only specifies when the landing should be initiated. It has been suggested that smooth decelerations can be achieved by controlling the rate of change of *Tau* with time, a quantity that has been termed *Taudot* (21). It can be shown (ref. 21 and *SI Appendix*, Text S6) that the constant-*Taudot* control principle leads to landing trajectory profiles that are described by an expression of the general form

$$V = Cz^{p+1}, \qquad [4]$$

where $V$ is the approach speed, $z$ is the target distance, $C$ is a constant that is determined by the initial conditions of the landing trajectory, and $p$ is a parameter that specifies the value of *Taudot*—the rate at which *Tau* is varied. Because *Tau* can be measured as indicated above (ratio of image size to rate of expansion), the rate of change of this quantity can also be monitored, in principle, and its variation in time can be controlled as required by varying the speed of approach.

**The Constant-*Tau* Model of Visual Guidance for Landing.** In the constant-*Taudot* model, the relationship between approach velocity $V$ and target distance $z$ depends upon the value of $p$ (*SI Appendix*, Fig. S5*A*). Plots of $V$ against $z$ are concave-upward for $P > 0$ (*Tau* increases with time), convex-upward for $P < 0$ (*Tau* increases with time), and linear for $P = 0$ (*Tau* is invariant with time). The linear relationship that we have observed between $V$ and $z$ for stationary spirals (Figs. 3 and 4) indicates that honey bee landings can be described within the *Taudot*-control framework as a special case in which *Tau*, the projected time to contact (abbreviated as PTTC), is held constant ($P = 0$). We call this the "constant-*Tau*" strategy.

For the case of $P = 0$, Eq. **4** reduces to

$$\frac{V}{z} = C, \qquad [5]$$

which has exactly the same form as Eq. **2**, where the right-hand side is also constant. From the standpoint of *Taudot*-controlled guidance of landings, the special case of constant-*Tau* control is particularly simple to implement because it does not require explicit computation of the PTTC or its rate of change; it only entails measurement of the rate of expansion of the image, and adjustment of the speed of approach to hold this rate of expansion constant.

In *SI Appendix*, Text S6 we derive theoretically how the rate of image expansion (plotted as the angular velocity in a 45° viewing direction) would vary with distance from the target, for various values of $p$ in the constant-*Taudot* model (*SI Appendix*, Fig. S5*B*). For positive values of $p$ the angular velocity would decrease to a value of zero as the target is approached (*Tau* increased with time, blue curve). For negative values of $p$ the angular velocity would increase to very high values as the target is approached (*Tau* decreases with time, red curve). When $P = 0$ (which represents constant-*Tau* control), the angular velocity would remain constant throughout the landing trajectory (*Tau* is invariant with time, black curve). This is exactly what we observe in the experiments with the stationary and the expanding spirals (Fig. 3*B*). This finding lends additional support to the model of constant-*Tau* guidance for landing.

Van Breugel and Dickinson (6) examined the variation of approach speed with target distance when *Drosophlia* land on a vertical post. They find that, unlike the findings of our present study, the approach speed is not proportional to target distance. Rather, it is approximately proportional to the logarithm of target distance (figure 8A in ref. 6). One reason for the discrepancy between their finding and ours could be due to differences in insect order (Diptera versus Hymenoptera). Another explanation could be that their flies approached a cylindrical surface, whereas our bees approached a plane surface. When approaching a cylinder, the instantaneous angle that the cylinder subtends in the eye of the approaching insect is not the angle subtended by its diameter. Rather, it is the angle subtended by the tangents to the circular cross-section of the cylinder. If this is taken into account, one would expect the rate of image expansion generated by the cylinder to be progressively greater than that generated by a plane surface as the insect moves closer to the target. In this situation, our model predicts that the curve of approach speed would have a nonlinear, convex-upward profile when plotted against a linear distance axis, which approximates a linear relationship when plotted against a logarithmic distance axis (*SI Appendix*, Text S7 and Fig. S6*B*). Thus, our model explains their data at least in a qualitative sense.

## Conclusion

Our experimental results and modeling reveal a simple strategy for accomplishing smooth landings on vertical surfaces. The results described here indicate that, when landing on a vertical surface, honey bees control the speed of their flight by holding constant

a particular measure of the magnitude of the optic flow profile that is generated by the surface. This automatically ensures that the flight speed is reduced gradually as the surface is approached and reaches a value close to zero just before touchdown, enabling smooth and safe landings. This strategy can be applied to landing on surfaces of any orientation, as well as on a variety of other 3D objects such as ridges or flower-like structures.

## Methods

The experiments were carried out in an indoor facility at the Australian National University in Canberra, Australia. The temperature inside the facility was maintained at 24 ± 5 °C during the day. A hive mounted on the wall supplied the honey bees (*Apis mellifera ligustica*) used in the experiments.

The apparatus (*SI Appendix*, Fig. S1) consisted of a vertically oriented Perspex disk, 60 cm in diameter. The disk was attached to a variable speed dc motor, which was operated remotely by an electronic controller. The motor allowed the disk to be rotated clockwise or counterclockwise at a rate of up to two rotations per second. A plastic tube, 1.5 cm in diameter, was positioned at the center of the disk for the honey bees to land on. The tube ran through the center of the motor to the back of the apparatus, where it was attached to a small black Perspex box containing a sugar-water feeder. The disk was covered from the front with a transparent Perspex shield, which prevented any air currents that might be generated by the motion of the disk.

The experiments took place within a 1.5- × 1.5- × 1.5-m cage of black insect netting that bees could enter via a 15- × 15-cm rectangular hole positioned 1.2 m from the center of the landing apparatus. Honey bees were trained to enter the flight cage and to land on the tube at the center of the experimental apparatus. After landing, they could crawl through the tube to collect sugar water from a feeder at the rear of the apparatus. Each trained bee was marked with paint for individual identification except in Exp. 3, in which individual identity was not recorded. Bees were allowed to visit the feeder for 48 h before the experiments began, during which time the control pattern (Exp. 1, checkerboard; Exps. 2 and 3, four-arm spiral) was displayed on the disk.

The visual stimuli used in Exp. 1 were a black-and-white checkerboard pattern with a check size of 3.5 cm (Fig. 2*A*, *Inset*), a pattern of concentric black-and-white 3.5-cm-wide rings (Fig. 2*B*, *Inset*), and a pattern of 12 black-and-white evenly spaced sectors (Fig. 2*C*, *Inset*). All patterns were 60 cm in diameter.

The effects of changes in the speed of radial expansion cues on the landing response of honey bees were investigated using a black-and-white spiral pattern, 60 cm in diameter (Exp. 2). The black and white areas of the spiral were equal in size and number (four black and four white arms; *SI Appendix*, Fig. S1*C*). The radius of each contrast border (or arm) on the spiral increased exponentially, with a pitch value of 0.3, with the angle from the center ensuring that the profile of optic flow generated by rotating the spiral is the same as that which would be generated on the approach to the spiral when it was stationary (*SI Appendix*, Text S2).

The effect of changes in radial expansion on landing was examined by recording approaches to the spiral pattern when it was stationary and when it was rotating either clockwise (increasing the rate of radial expansion) or counterclockwise (decreasing the rate of radial expansion) at 0.5 and 1.0 rps. The experimental conditions were presented in a randomized order over a period of 4 d with the full set of experimental conditions being presented each day.

The effect of temporal frequency on the landing responses of honey bees was investigated using three spiral patterns (Exp. 3), each with three, four, or six arms (*SI Appendix*, Fig. S1*C*). The properties of the spirals were otherwise the same as those of the pattern used in Exp. 2. Landing approaches to each spiral pattern were recorded when it was stationary and when it was expanding or contracting at 1.0 rps. Bees were allowed to visit the stationary four-arm spiral for 48 h before the experiment took place. Each 30-min testing period was followed by a 30-min control period during which the stationary four-arm spiral was displayed and bees continued to visit the feeder. The experimental conditions, in which both the spiral pattern and the speed and direction of pattern rotation were varied, were presented in a randomized order over a period of 5 d, with the full set of experimental conditions being presented each day. Note that each of the three experiments was conducted independently using a separate group of trained bees.

The approach flights of honey bees to the apparatus were filmed at a rate of 400 Hz using two synchronized high-speed cameras (MotionPro 10k; Redlake, Inc.). Bee position was tracked in image sequences from each camera using a program developed in Matlab (The MathWorks, Inc.) and reconstructed in 3D using the camera calibration toolbox for Matlab (22).

Speed in each flight was determined by calculating the change in the perpendicular distance between the bee and the vertical plane of the disk over time ($z$ axis; *SI Appendix*, Fig. S2). Preliminary analyses revealed that the lateral and vertical components of flight velocity were much smaller in magnitude compared with that of the axial component (Fig. 1). The axial component of flight velocity therefore provided a good approximation of the actual magnitude of the approach speed. Speed data were estimated from linear interpolations at 2-mm intervals between 75 and 300 mm from the pattern to enable averaging at specified distances.

Linear mixed model analyses (23) using the lme function in R (R Foundation for Statistical Computing) were developed to test for the influence of including multiple flight data from individual bees as well as the effect of time, temperature, light intensity, and humidity. The variation between flights of the same bee was found to be similar to the variation of flights of different bees, indicating that each flight represented, in effect, an independent data point. The effects of the covariates were not significant and were therefore not considered in the final analyses. Linear models (lm function in R) were fitted using the least-squares method.

**ACKNOWLEDGMENTS.** We thank Paul Helliwell and Judith Reinhard for their assistance with the experiments and the anonymous referees for their suggestions for improving the manuscript. This work was supported by Australian Research Council (ARC) Centre of Excellence in Vision Science Grant CE0561903, ARC Discovery Grant DP0559306, US Asian Office of Aerospace Research and Development Grant FA4869-07-1-0010, and by a Queensland Government Premier's Fellowship.

1. Borst A (1986) Time course of the housefly's landing response. *Biol Cybern* 54(6): 379–383.
2. Borst A, Bahde S (1988) Spatio-temporal integration of motion. *Naturwiss* 75(5): 265–267.
3. Goodman LJ (1960) The landing responses of insects: I. The landing response of the fly, Lucilia sericata, and other Calliphorinae. *J Exp Biol* 37(4):854–878.
4. Srinivasan MV, Zhang S, Chahl JS (2001) Landing strategies in honeybees, and possible applications to autonomous airborne vehicles. *Biol Bull* 200(2):216–221.
5. Srinivasan MV, Zhang SW, Chahl JS, Barth E, Venkatesh S (2000) How honeybees make grazing landings on flat surfaces. *Biol Cybern* 83(3):171–183.
6. van Breugel F, Dickinson MH (2012) The visual control of landing and obstacle avoidance in the fruit fly Drosophila melanogaster. *J Exp Biol* 215(Pt 11):1783–1798.
7. Wagner H (1982) Flow-field variables trigger landing in flies. *Nature* 297(5862): 147–148.
8. Wehrhahn C, Hausen K, Zanker JM (1981) Is the landing response of the housefly (*Musca*) driven by motion of a flowfield? *Biol Cybern* 41(2):91–99.
9. Lee DN, Davies MNO, Green P, van Der Weel FR (1993) Visual control of velocity of approach by pigeons when landing. *J Exp Biol* 180(1):85–104.
10. Davies MNO, Green PR (1990) Optic flow-field variables trigger landing in hawk but not in pigeons. *Naturwissenschaften* 77(3):142–144.
11. Srinivasan MV (1993) How insects infer range from visual motion. *Rev Oculomot Res* 5(2):139–156.
12. Collett TS, Harkness LIK (1982) Depth vision in animals. *Analysis of Visual Behavior*, eds Ingle DJ, Goodale MA, Mansfield RJW (MIT Press, Cambridge, MA), pp 111–176.
13. Burkhardt D, Darnhofer-Demar B, Fischer K (1973) Zum binokularen Entfernungssehen der Insekten. *J Comp Physiol* 87(2):165–188.
14. Edwards M, Ibbotson MR (2007) Relative sensitivities to large-field optic-flow patterns varying in direction and speed. *Perception* 36(1):113–124.
15. Koenderink JJ, van Doorn AJ (1976) Local structure of movement parallax of the plane. *J Opt Soc Am* 66(7):717–723.
16. Evangelista C, Kraft P, Dacke M, Reinhard J, Srinivasan MV (2010) The moment before touchdown: Landing manoeuvres of the honeybee Apis mellifera. *J Exp Biol* 213(2): 262–270.
17. Srinivasan MV, Lehrer M, Kirchner WH, Zhang SW (1991) Range perception through apparent image speed in freely flying honeybees. *Vis Neurosci* 6(5):519–535.
18. Srinivasan M, Zhang S, Lehrer M, Collett T (1996) Honeybee navigation en route to the goal: Visual flight control and odometry. *J Exp Biol* 199(Pt 1):237–244.
19. Si A, Srinivasan MV, Zhang S (2003) Honeybee navigation: Properties of the visually driven 'odometer'. *J Exp Biol* 206(Pt 8):1265–1273.
20. Baird E, Srinivasan MV, Zhang S, Cowling A (2005) Visual control of flight speed in honeybees. *J Exp Biol* 208(Pt 20):3895–3905.
21. Lee DN, Kalmus H (1980) The optic flow field: The foundation of vision. *Philos Trans R Soc Lond B Biol Sci* 290(1038):169–179.
22. Bouguet J-Y (1999) Visual methods for three-dimensional modelling. PhD thesis (California Inst of Technology, Pasadena, CA).
23. McCulloch CE, Searle SR (2001) *Generalized, Linear, and Mixed Models* (Wiley, New York).